Annals of R.S.C.B., ISSN:1583-6258, Vol. 25, Issue 3, 2021, Pages. 5674 - 5708
Received 16 February 2021; Accepted 08 March 2021.

Spectroscopic investigation and molecular docking analysis of 5- (4-Chlorobenzylidene)-2-{3-(4-chlorophenyl)-5-[4-(propan-2-yl) phenyl]-4, 5-dihydro-1*H*-pyrazol-1-yl}-1, 3-thiazole-4(5*H*)-one

J Jayasudha[a], V Balachandran[a,*]

[a]Centre for Research – Department of Physics, Arignar Anna Government Arts College, Musiri, (Affilated to Bharathidasan University), Tiruchirappalli, India 621 211

Abstract

The targeted molecular structure of 5-(4-Chlorobenzylidene)-2-[3-(4-chlorophenyl)-5-[4-(propan-2-yl)phenyl]-4-5-dihydro-1*H*-pyrazol-1-yl]-1,3-thiazole-4(5*H*)-one have been determined and analyses by DFT method employing CAM-B3LYP/6-31G(d,p) and B3LYP/6-311G (d, p) level of theory. Theoretically calculated geometric parameters were compared with experimental (XRD) data. Based on local reactivity descriptor such as HOMO-LUMO energy gap, electrostatic potential were calculated and deliberated. On the basis of potential energy distribution (PED) by VEDA software, the scaled values of the calculated normal modes of vibration frequencies (FT-IR and FT-Raman) were assigned and compared with experimentally observed one. Natural bond orbital (NBO) analysis of the title molecule was studied. Docking analysis revealed that the title compound (Ligand) has strong binding affinity against protein for antibacterial, anti-cancer and anti-fungal activities. The ligand forms a stable complex with the proteins and recommended further analysis on present compound for their in-depth biological and pharmaceutical consequence.

Keyword: DFT, Molecular Docking, NBO, Anti-tumor

1. Introduction

In recent years, Pyrazole – thiazolee established a class of heterocyclic compound which contains oxygen, nitrogen and sulphur atoms. This organic molecule has exhibit imposing importance in medicinal and chemical applications. These heterocyclic compounds and their derivatives have good anti-cholinesterase, anti-cancer, anti-analgesic and anti-inflammatory activities [1-3]. The five-membered nitrogen linked heterocyclic compounds were widely applied as cosmetics, food additives, agrochemicals, bio-mimetic catalysts, optical brighteners, laser,

Annals of R.S.C.B., ISSN:1583-6258, Vol. 25, Issue 3, 2021, Pages. 5674 - 5708
Received 16 February 2021; Accepted 08 March 2021.

fluorescent and dyes [4-6]. Various thiazolee based pharmaceutical drugs have been playing indispensable role for the diagnosis of different types of syndromes and generate potential to synthesis new thiazolee derivatives with biological influence were actively oppressed worldwide. Due to the broad therapeutic properties of thiazolee derivatives, chemists have interest to synthesize a colossal number of novel chemotherapeutic agents in the medicinal field [7]. Recently I.Azad et al [8] reported pyrazole moity have anti-tumor behavior against hepato-cellular carcinoma (liver disease) which is only treated by non- surgical methods [9]. Some pyrazole-thiazolee derivatives have antibacterial, antiviral, insecticidal and fungicidal activities [10-15]. For drug design, computational studies make an essential role before experimental validation in laboratory and farther clinical trials leading to avoid loss of money and time. Now-a-days pyrazole - thiazoleidinone derivatives were very much useful to improve in drug design. Influenced by the above mentioned applications, the present molecule 5-(4-chlorobenzylidene)-2-[3-(4-chlorophenyl)-5-[4-(propan-2-yl)phenyl]-4-5-dihydro-1*H*-pyrazol-1-yl]-1, 3-thiazole-4(5*H*)-one has chosen for the computational studies and evaluated spectroscopic features, structural properties, also focus on the potent of antibacterial, anticancer and antifungal agents using computational stimulated methodology. The binding affinity to the receptor of the molecule has predicted by docking to form a stable complex with least energy of binding. MEP analysis to affirm reactive sites and chemical reactivity parameter attained through molecular orbital analysis. Density functional theory has been widely used for various quantum chemical calculations to achieve above consequence. In the present study, theoretical calculations of spectral and structural parameters have been explore through DFT/B3LYP/6-31G (d,p) and 6-311G (d,p) level of methods. Through the literature survey, there are no reported studies on the title compound using DFT method.

2. Experimental and computational procedures

The molecular structure of 5-(4-Chlorobenzylidene)-2-[3-(4-chlorophenyl)-5-[4-(propan-2-yl) phenyl]-4-5-dihydro-1*H*-pyrazol-1-yl]-1,3-thiazole-4(5*H*)-one was synthesized as per the procedure reported in Salian et al.[16] with melting point $282-284°C$. The experimental data of FT-IR and FT-Raman spectra were recorded in solid phase at room temperature. The FT-IR spectrum of the compound have been recorded in the range 4000-450 cm^{-1} using Perkin Elmer spectrometer with KBr pellet technique, while FT-Raman spectrum has recorded by Nd-YAG

Annals of R.S.C.B., ISSN:1583-6258, Vol. 25, Issue 3, 2021, Pages. 5674 - 5708
Received 16 February 2021; Accepted 08 March 2021.

laser source having 1064nm wavelength in the range 4000-0 $cm^{-1}$and these spectral data have been compiled at SAIF (Sophisticated Analytical Instruments Facility), IIT Chennai, India.

The quantum chemical calculations were performed by Gaussian 09W[17] and Gauss view software[18] at CAM-B3LYP/6-31G(d,p) and B3LYP/6-311G(d,p) basis set using DFT method. With the Becke's three parameter hybrid functional (B3) [19,20] with Lee-Yang-Parr (LYP) correlation function [21] of DFT method was approved due to its cost efficiency and exemplary correctness in occurring observed value for geometrical parameter and vibrational frequencies. The vibrational assignments were done according to their Potential Energy Distributions (PEDs) by VEDA (Vibrational Energy Distribution Analysis) program [22] and visualization from Gauss view [18]. The charge distribution of the title compound was summarized by molecular electrostatic potential and HOMO-LUMO to examine the neucleophilic and electrophilic regions for the compound in three dimensions with help of TD-DFT. The molecular docking study has also investigated by Auto Dock Tools [23] and the visual representations of protein–Ligand complex were obtained via PyMol interface and in Discovery Studio 4.1 [24].

3. Result and Discussion

3.1 Description of molecular structure

The optimized structure of the title compound is given along with atom labeling scheme as shown in Figure 1. The geometry parameters such as bond length and bond angle were computed by DFT method using B3LYP/6-311G (d, p). Table 1 displays the optimized geometry parameter of 5-(4-Chlorobenzylidene)-2-[3-(4-chlorophenyl)-5-[4-(propan-2-yl) phenyl]-4-5-dihydro-1*H*-pyrazol-1-yl]-1,3-thiazole-4(5*H*)-one molecule belongs to C1 point group symmetry. The experimental values are correlated well with theoretical value; however some of the calculated values of the compound have slightly varied from experimental values. The phenyl ring C-C bond length lies in the range of 1.40-1.38 Å for MPDIA, 1.49-1.39 Å for BPDIA [25]. In addition, for ‘chloro’ substitution of PBA the C-C bond length observed in the range of 1.39 - 1.36 Å and calculated values were in the range 1.40-1.39 Å [26]. In this case the calculated bond length are C10-C11, C20-C21, C20-C28, C23-C25, C25-C26, C48-C49, C48-C50, C49-C51, C50-C53, C51-C55, C53-C55 ≈ 1.40 Å, C10-C18, C11-C13, C13-C15, C15-C16, C16-C18, C21-C23, C26-C28 ≈ Å. The substituted methyl groups of the carbon bond length of the title compound are C30-C32 and C30-C36 is 1.53 Å, which are slightly vary with experimental value

Annals of R.S.C.B., ISSN:1583-6258, Vol. 25, Issue 3, 2021, Pages. 5674 - 5708
Received 16 February 2021; Accepted 08 March 2021.

as 1.51 Å. Due to the electron displacement by the external field and an induced dipole moment is produced which changes when the bond length changes during the molecular vibration. While the bond length of C4-C6 ≈1.55 Å, C4-C20, C6-C9 and C41-C42 ≈ 1.51 Å, C9-C10 ≈ 1.50 Å were elongated due to the transfer of a lone pair of electrons [27]. The halogen substituted carbons of Cl1-C15 and C55-Cl58 bond length is 1.74 Å and 1.76 Å [28]. The bond length of N-C single bond is N2-C4 ≈ 1.48 Å, N2-C40≈1.47 Å, and N3-C9≈1.28 Å which are well agree with experimental value [29-31].

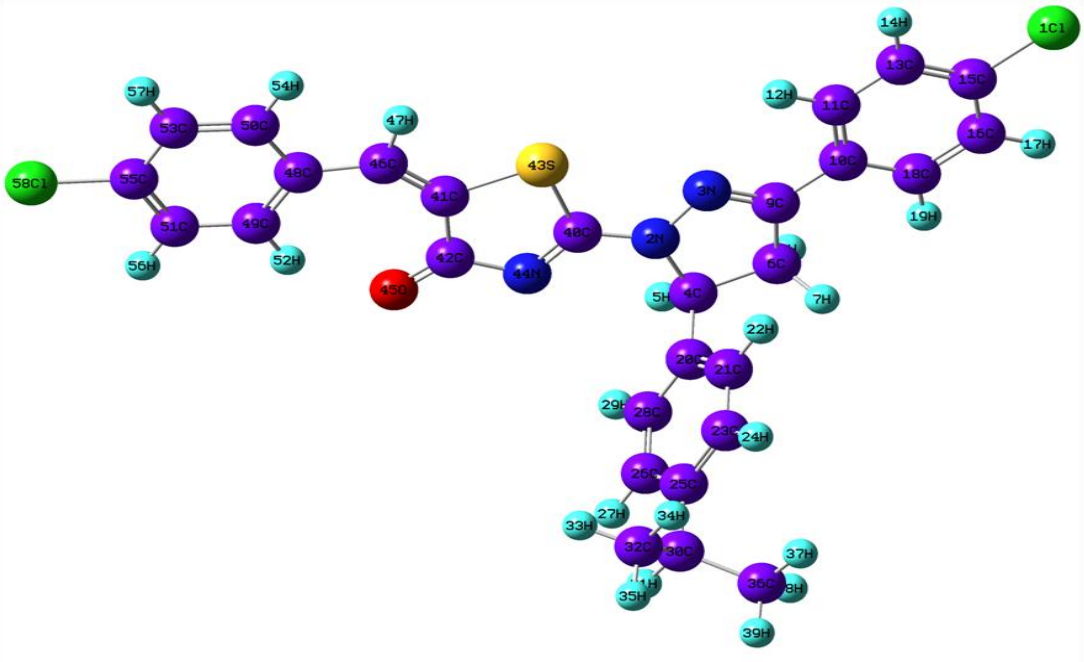

Figure 1. Molecular structure of 5-(4-Chlorobenzylidene)-2-[3-(4-chlorophenyl)-5-[4-(propan-2-yl) phenyl]-4-5-dihydro-1*H*-pyrazol-1-yl]-1, 3-thiazole-4(5*H*)-one

Table 1: optimized Geometrical parameter of 5-(4-Chlorobenzylidene)-2-[3-(4-chlorophenyl)-5-[4-(propan-2-yl) phenyl]-4-5-dihydro-1H-pyrazol-1-yl]-1,3-thiazole-4(5H)-one: bond length (Å)

Label	DFT Value	XRD	Label	DFT Value	XRD	Label	DFT Value	XRD
Cl1-C15	1.7435	1.7402	C18-H19	0.9503	0.9310	C40-S43	1.7765	1.7521
N2-N3	1.3812	1.3861	C20-C21	1.3947	1.3797	C40-N44	1.2955	1.2971
N2-C4	1.4889	1.4845	C20-C28	1.3929	1.3756	C41-C42	1.5144	1.5168
N2-C40	1.4701	1.3571	C21-H22	0.9496	0.9306	C41-S43	1.7900	1.7890

Annals of R.S.C.B., ISSN:1583-6258, Vol. 25, Issue 3, 2021, Pages. 5674 - 5708
Received 16 February 2021; Accepted 08 March 2021.

N3-C9	1.2823	1.2725	C21-C23	1.3842	1.3891	C41-C46	1.3500	1.3401
C4-H5	0.9997	0.9971	C23-H24	0.9505	0.9299	C42-N44	1.3593	1.3719
C4-C6	1.5461	1.5461	C23-C25	1.394	1.3603	C42-O45	1.2155	1.2156
C4-C20	1.5136	1.5079	C25-C26	1.3954	1.3828	C46-H47	0.9965	0.9300
C6-H7	0.9901	0.9699	C25-C30	1.5159	1.5156	C46-C48	1.4609	1.4601
C6-H8	0.9899	0.9701	C26-H27	0.9495	0.9305	C48-C49	1.4083	1.3904
C6-C9	1.5105	1.5099	C26-C28	1.3823	1.3927	C48-C50	1.4106	1.3936
C9-C10	1.4709	1.4582	C28-H29	0.9500	0.9300	C49-C51	1.3888	1.3800
C10-C11	1.4046	1.3923	C30-H31	1.0007	0.9803	C49-H52	0.9904	0.9300
C10-C18	1.3870	1.3837	C30-C32	1.531	1.4307	C50-C53	1.3868	1.3774
C11-H12	0.9499	0.9292	C30-C36	1.5245	1.4354	C50-H54	0.9987	0.9301
C11-C13	1.3862	1.3825	C32-H33	0.9796	0.9584	C51-C55	1.3913	1.3886
C13-H14	0.9497	0.9301	C32-H34	0.9795	0.9592	C51-H56	0.9897	0.9302
C13-C15	1.3833	1.3631	C32-H35	0.9801	0.9602	C53-C55	1.3910	1.3895
C15-C16	1.3753	1.3676	C36-H37	0.9806	0.9597	C53-H57	0.9908	0.9300
C16-H17	0.9504	0.9307	C36-H38	0.98	0.9606	C55-Cl58	1.7579	1.7440
C16-C18	1.389	1.3728	C36-H39	0.98	0.9605			

3.2 Spectral analysis

The molecular structure of 5-(4-Chlorobenzylidene)-2-[3-(4-Chlorophenyl)-5-[4-(propan-2-yl) phenyl]-4-5-dihydro-1*H*-pyrazol-1-yl]-1,3-thiazole-4(5*H*)-one has 58 atoms of 168 normal vibration modes. The FT-IR and FT-Raman vibrational assignments of the studied compound were performed on the basis set of harmonic force field calculations at CAM-B3LYP/6-31G (d,p) and B3LYP/6-311G(d,p) level. Table 2 shows the comparison of experimental and theoretical frequency band assignments with potential energy distribution (PED) and the compared IT and Raman spectra were displayed in figure 2 and 3 respectively. From the result of computed vibration frequencies are slightly differ from experimentally observed one.

Annals of R.S.C.B., ISSN:1583-6258, Vol. 25, Issue 3, 2021, Pages. 5674 - 5708
Received 16 February 2021; Accepted 08 March 2021.

Carbon-Hydrogen vibration

The C-H stretching vibrations in hetro aromatic structure exhibit in the range of 3100-2900cm^{-1}[32] and this occurrence clear identification of the structure. In this present work, the C-H stretching vibration observed at 3061cm^{-1} in IR spectrum and at 3065 cm^{-1} in FT-Raman spectrum. The calculated values of C-H stretching bands are 3071, 3063, 3058, 3054, 3049, 3046, 3039, 3027, 3019, 3008, 2999, 2992, 2976 cm^{-1} with CAM-B3LYP/6-31G(d,p) and at 3064, 3059, 3054, 3051, 3047, 3042, 3038, 3021, 3012, 3003, 2997, 2988, 2980, 2972 cm^{-1} with PED range from 96-98% by B3LYP/6-311G(d,p) method. For aromatic ring C-H in-plane-bending and out-of plane bending vibrations are appeared in the range 1500-700cm^{-1} through literature [33]. The C-H in-plane-bending mode has observed at 1327, 1087cm^{-1} in IR spectrum and at 1333, 1285, 1250, 1089 cm^{-1} in FT-Raman spectrum. Theoretically calculated values of C-H in-plane bending mode were obtained at 1465, 1452, 1441, 1355, 1343, 1332, 1323, 1309, 1294, 1287, 1265, 1260, 1251, 1165, 1153, 1107, 1098, 1091cm^{-1} with CAM-B3LYP/6-31G (d, p) level. By B3LYP/6-311G(d,p) level this vibration bands have been assigned at 1461, 1448, 1439, 1353, 1341, 1330, 1318, 1304, 1290, 1284, 1263, 1258, 1250, 1214, 1163, 1150, 1105, 1195, 1088 cm^{-1}. Additionally C-H out-of-plane bending mode in aromatic ring have been determined at 952, 897, 747 cm^{-1} in FT-IR and at 950, 748 cm^{-1} in Raman spectrum. The computed C-H(out-of-plane) bending mode were obtained at 954, 945, 931, 919, 905, 899, 875, 835, 819-745, 296cm^{-1} and at 951, 941, 928, 917, 902, 895, 870, 832, 814-740, 292 cm^{-1} through CAM-B3LYP/6-31G (d,p) and B3LYP/6-311G(d,p) methods correspondingly. These assignments were supported by the literature survey [34-36].

CH_2 vibration

The asymmetric and symmetric CH_2 stretching vibrations were determined in the region 3000-2900 cm^{-1} and 2900-2800 cm^{-1} and also it exist at lower frequencies [27]. The computed CH_2 asymmetric and symmetric stretching vibration modes are assigned at 2957, 2953 cm^{-1} with

Annals of R.S.C.B., ISSN:1583-6258, Vol. 25, Issue 3, 2021, Pages. 5674 - 5708
Received 16 February 2021; Accepted 08 March 2021.

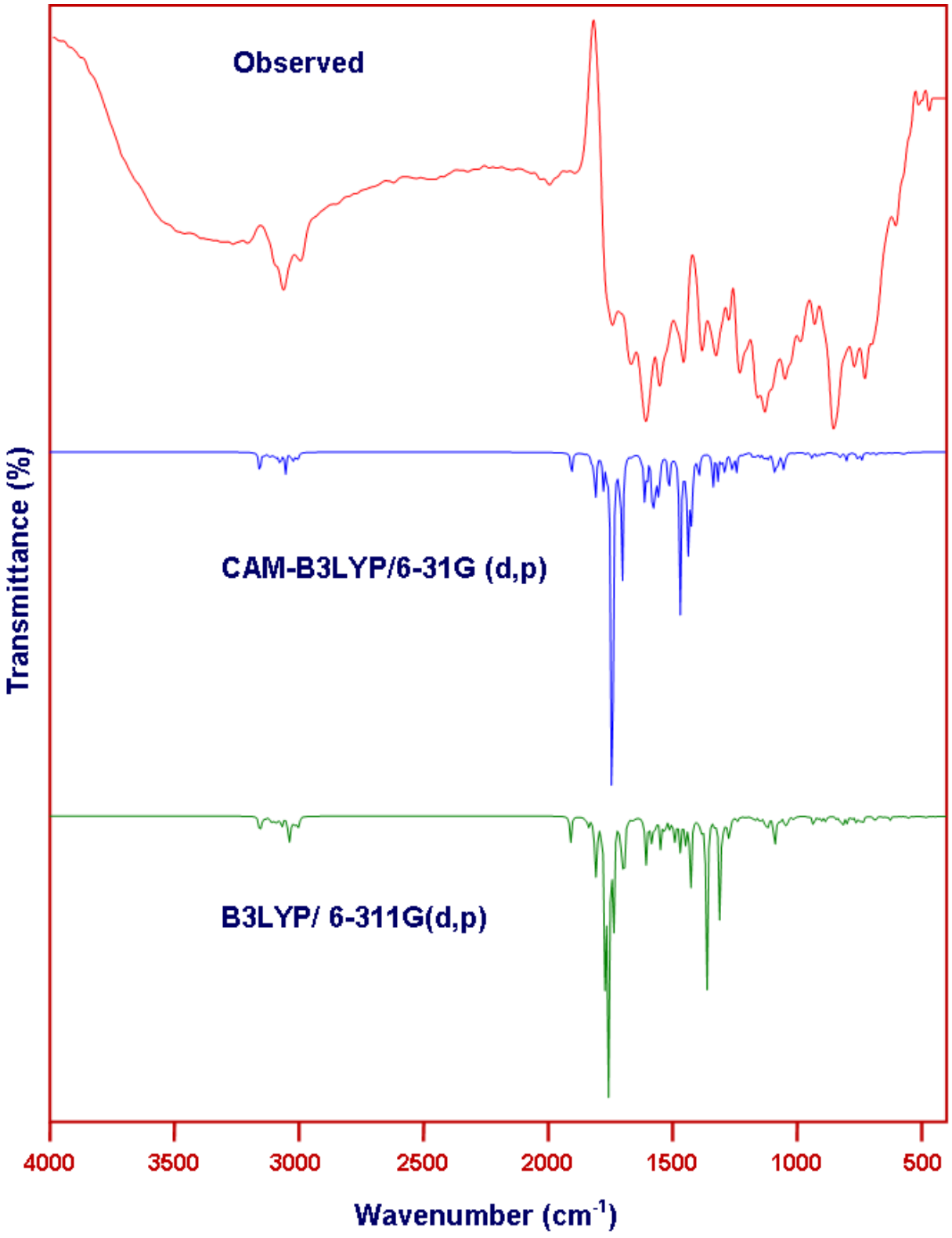

Figure 2. Observed and stimulated FT-IR spectrum of 5-(4-Chlorobenzylidene)-2-[3-(4-chlorophenyl)-5-[4-(propan-2-yl) phenyl]-4-5-dihydro-1*H*-pyrazol-1-yl]-1, 3-thiazole-4(5*H*)-one

Annals of R.S.C.B., ISSN:1583-6258, Vol. 25, Issue 3, 2021, Pages. 5674 - 5708
Received 16 February 2021; Accepted 08 March 2021.

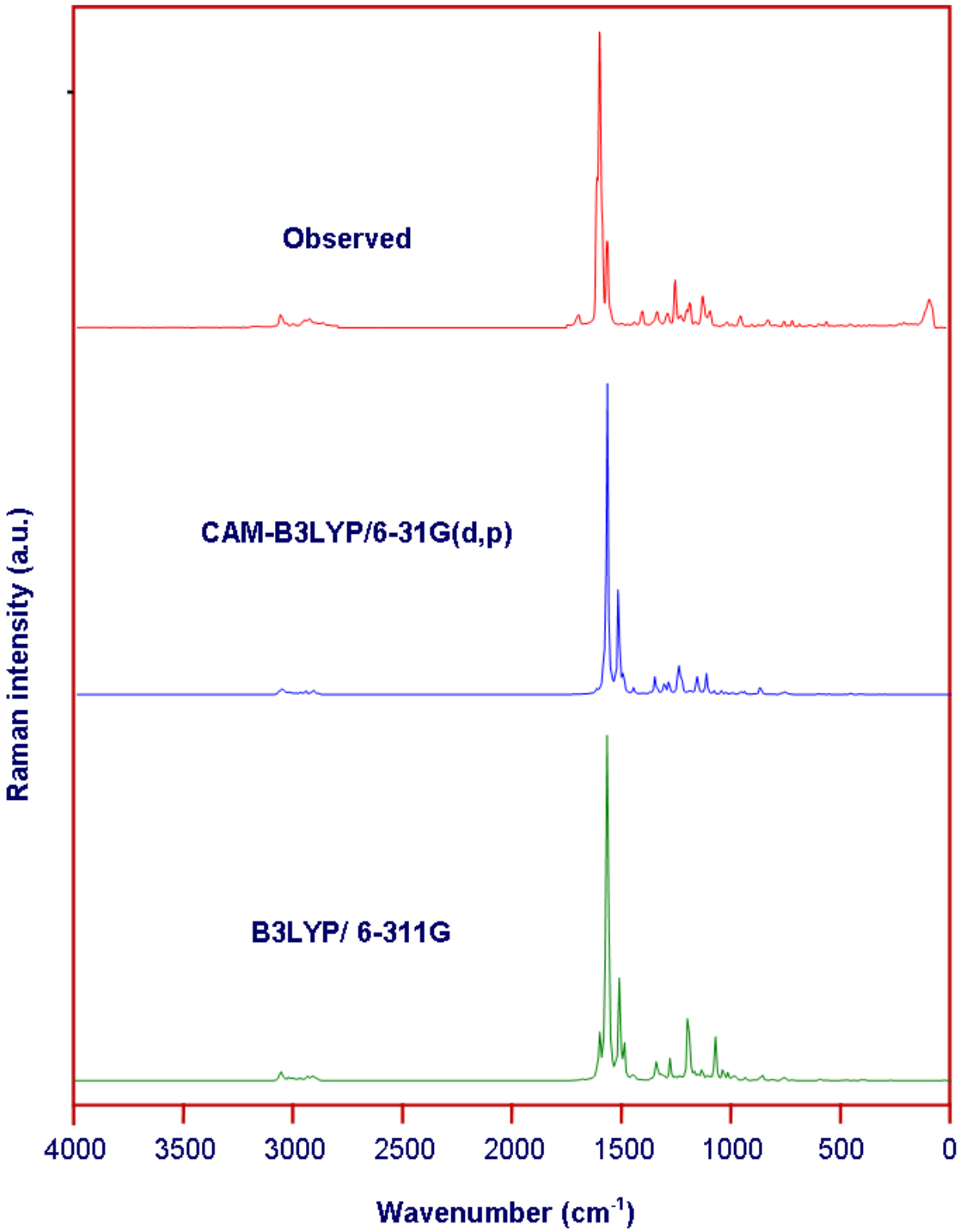

Figure 3. Observed and calculated FT-Raman spectrum of 5-(4-Chlorobenzylidene)-2-[3-(4-chlorophenyl)-5-[4-(propan-2-yl) phenyl]-4-5-dihydro-1*H*-pyrazol-1-yl]-1, 3-thiazole-4(5*H*)-one

PED 88% and at 2917, 2913cm^{-1} with PED 89% through CAM-B3LYP/6-31G (d,p) and

Annals of R.S.C.B., ISSN:1583-6258, Vol. 25, Issue 3, 2021, Pages. 5674 - 5708
Received 16 February 2021; Accepted 08 March 2021.

B3LYP/6-311G(d,p) methods. But experimentally recorded spectra does not exist any peak in these vibration bands. The CH_2 bending modes normally emerge in the region between 1450 and 875cm^{-1} [33]. The scissoring mode of CH_2 vibration is recorded at 1455 ± 55 cm^{-1} in FT-IR band [27]. In CH_2 group, the computed scissoring mode found at 1364, 1362 cm^{-1} with PED contribution 71%. The CH_2 rocking vibration is assigned at 1197 and 1195 cm^{-1} with PED 68%. The recorded band at 1123 cm^{-1} in FT-Raman spectrum determine to the CH_2 twist mode and the calculated wavenumber for this mode at 1125 and 1120 cm^{-1} with potential energy of 68%. CH_2 wagging vibration mode observed at 461cm^{-1} in FT-IR spectrum and computed wavenumber assigned at 465 cm^{-1} and 460 cm^{-1} with energy contribution of 62% by CAM-B3LYP/6-31G (d,p) and B3LYP/6-311G(d,p) methods.

Methyl group vibration

In general, CH_3 group associated to electron donating substitution in aromatic system [27, 37] and these vibrations are arises in the range 3000-2840 cm^{-1}. Asymmetric stretching vibration of methyl group assigned at 2968, 2946, 2934, 2925/2965, 2941, 2930, 2922 cm^{-1} by CAM-B3LYP/6-31G (d,p) and B3LYP/6-311G(d,p) levels. Similarly, the computed symmetric stretching of CH_3 group is found at 2909, 2895/2904, 2893 cm^{-1}. Normally, the symmetric and asymmetric bending vibration modes of methyl group emerging in the range 1355-1395 cm^{-1} and 1430-1470cm^{-1} [38]. The symmetric bending vibration have been observed at 1397 cm^{-1} in FT-IR and at 1401cm^{-1} in FT-Raman spectra and it has calculated at 1427, 1402, 1315, 1299/ 1422, 1400, 1311, 1297 cm^{-1}. The computed asymmetric bending vibration mode of methyl group assigned at 1394, 1387/1391, 1384 cm^{-1} with PED 67, 68%. The rotating mode of rocking CH_3 vibration mode is computed at 1056, 999/ 1054, 998cm^{-1} and the out-of-plane bending CH_3 band assigned at 890, 844/ 888, 840cm^{-1}. The CH_3 torsion vibration mode has fall below 500cm^{-1} [27,39] and it has assigned at 199, 192/ 197, 189 cm^{-1} theoretically by CAM-B3LYP/6-31G (d,p) and B3LYP/6-311G (d,p) methods. For the title compound the observed wavenumber were in agreement with computed ones.

Aromatic ring vibration

For the hetero aromatic molecular structure C-C and C=C stretching vibrations were assigned in the range of 1650-1430cm^{-1} and 1380-1280 cm^{-1} respectively [34,40]. In the aromatic ring vibration mode the form of substitution plays major role. FT-IR peaks of the title compound were observed at 1541, 1274, 1225, 1183, 1115cm^{-1} and FT-Raman bands at 1609, 1562,

Annals of R.S.C.B., ISSN:1583-6258, Vol. 25, Issue 3, 2021, Pages. 5674 - 5708
Received 16 February 2021; Accepted 08 March 2021.

1182cm^{-1}, which were attributed to C-C stretching vibration mode. Theoretically computed C-C stretching vibration mode have been found at 1611, 1578, 1567, 1562, 1543, 1526, 1488, 1278, 1272, 1235, 1228, 1207, 1189, 1183, 1174, 1118cm^{-1} by CAM-B3LYP/6-31G(d,p) and at 1610, 1575, 1566, 1560, 1540, 1522, 1486, 1275, 1269, 1234, 1225, 1202, 1188, 1180, 1171, 1114 cm^{-1} through B3LYP/6-311G (d,p) level. The observed and theoretically computed values of C-C stretching vibration were congruence with reported values. Slightly differ from the expected range of values due to the substitution along with interface cause by C-N which happens to fall lower range. The C-C in-plane and out-of-plane bending vibrations were obtained in the range of 600-250 cm^{-1} and 560-420cm^{-1} [34, 41]. In the present structure C-C in-plane bending mode has observed at 589cm^{-1} in FT-IR spectrum and computed values at 994, 989, 985, 978, 967, 592, 407, 398, 176, 78, 73 cm^{-1} through CAM-B3LYP/6-31G (d,p) and at 991,988, 982, 973, 963, 588, 403, 394, 170, 74, 71cm^{-1} through B3LYP/6-311G (d,p) methods. Out -of –plane C-C bending vibration has observed at 825 cm^{-1} and 823, 81 cm^{-1} in FT-IR and FT-Raman spectra and theoretically calculated value are 827, 362 ,308, 285, 278, 272, 235, 219, 208, 184, 86cm^{-1}, at 825, 320, 304, 281, 275, 269, 230, 217, 203, 179, 80 cm^{-1} through same basis methods. The calculated CC torsion vibration mode has to be assigned at 69, 56, 47, 36, 31, 27, 24, 21, 19, 10cm^{-1} and 68, 50, 45, 31, 28, 25, 21, 20, 16, 8cm^{-1}. Below 500cm^{-1} wavenumber have been found to ring in-plane (δ_{ring}) and ring out-of-plane (γ_{ring}) bending vibration modes [34, 41, 42]. The observed ring in-plane vibration is at 554cm^{-1} in FT-Raman spectrum and the computed values are 734, 726, 687, 579, 572, 567, 559, 426, 265, 97cm^{-1} and at 731, 720, 681, 575, 570, 563, 555, 422, 260, 91cm^{-1} by CAM-B3LYP/6-31G(d,p) and B3LYP/6-311G(d,p) methods. A band observed at 706cm^{-1} in FT-IR is assigned to γ_{ring} vibration and corresponding computed vibrations at 710, 672, 648, 624, 597, 541, 495, 448, 441, 371, 356, 335, 141, 117, 109cm^{-1} and at 705, 668, 643, 619, 594, 538, 491, 444, 439, 369, 353, 332, 137, 112, 103 cm^{-1} by both CAM-B3LYP/6-31G(d,p) and B3LYP/6-311G(d,p) methods and these values are congruence with the literature.

C=O vibration

The most characteristic vibration mode of the IR and FT-Raman spectra has been C=O (ketones) vibration mode for the subjected molecular structure, which occurs in the range of $1725 \pm 65 cm^{-1}$[43, 44]. The observed C=O stretching band at 1668 cm^{-1} in FT-IR spectrum for

Annals of R.S.C.B., ISSN:1583-6258, Vol. 25, Issue 3, 2021, Pages. 5674 - 5708
Received 16 February 2021; Accepted 08 March 2021.

the title compound. Theoretically $\nu(C=O)$ band were obtained at 1669 and 1667cm^{-1} with PED contribution of 85% for CAM-B3LYP/6-31G (d,p) and B3LYP/6-311G (d,p) basis set and it has exemplary synchronize with the experimental wavenumber. The reported $\nu(C=O)$ vibration band for the synthesized title compound observed at 1666 cm^{-1}in FT-IR spectrum [16]. Murthy et al.[45] reported that at 1668cm^{-1} (IR), 1680cm^{-1}(Ra), 1679, 1678cm^{-1} (DFT) and at 1689 cm^{-1}(IR)of stretching mode in venil et al.[46]. An observed band at 711cm^{-1} in FT-Raman has corresponds to out-of-plane bending mode with PED 62%, while the vibration bending mode located at 719 and 712 cm^{-1} theoretically by both CAM-B3LYP/6-31G (d,p) and B3LYP/6-311G (d,p) methods. The reported values of $\gamma(C=O)$ vibration mode were 679, 662 cm^{-1}(IR), 658, 551cm^{-1} (Ra), 678, 667, 553 cm^{-1} (DFT) [45], 606, 569 cm^{-1} (DFT) [47], at 753cm^{-1} (IR), 755, 751, 748, 745cm^{-1} (DFT)[46].

C-Cl vibration

The C-Cl vibration modes are obtainable due to the lowering of molecular symmetry and heavy atoms being on the molecular structure. In general, the frequency range of 1129-480cm^{-1} assigned to the C-X group (X- Cl, F, Br, I) vibration [27, 35]. In the present work, the stretching vibration mode between chlorine and phenyl ring is observed at 1010 cm^{-1} in FT-IR, 1037, 1033, 1015, 1011 cm^{-1} with PED contribution of 68% theoretically by CAM-B3LYP/6-31G (d,p) and B3LYP/6-311G (d,p) methods correspondingly. However the strong absorption vibration bands between chlorine and aromatic ring, there is a shift might be occurs as high as 840cm^{-1} [48]. The stretching C-Cl vibration band appears at 389, 386, 377, 375 cm^{-1} with PED 62% due to the long bond length the vibration mode fall into lower frequency. In –plane-bending vibration of C-Cl mode to be cited at 257, 253, 246, 241 cm^{-1} with 62% of potential energy distribution and for out-of-plane C-Cl bending mode assigned at 163, 159, 154, 148 cm^{-1} of 52% of PED contribution through CAM-B3LYP/6-31G (d,p) and B3LYP/6-311G (d,p) methods. The observed reported value of $\nu C-Cl$ mode at 829cm^{-1} (IR) in v.v.salian et al.[16], at 673cm^{-1} (Ra), 671cm^{-1} (DFT) in Beegum et al.[49]. Viji et al.[14] reported that observed $\nu C-Cl$ band at 414 cm^{-1} (IR), 416, 415 cm^{-1} (DFT) and at 311, 309 cm^{-1} of C-Cl in-plane-bending, at 155, 153 cm^{-1} (DFT) of C-Cl out-of-plane bending given by Sivakumar et al.[15].

Annals of R.S.C.B., ISSN:1583-6258, Vol. 25, Issue 3, 2021, Pages. 5674 - 5708
Received 16 February 2021; Accepted 08 March 2021.

Table 2: Observed and calculated scaled vibration wavenumbers of 5-(4-Chlorobenzylidene)-2-[3-(4-chlorophenyl)-5-[4-(propan-2-yl) phenyl]-4-5-dihydro-1H-pyrazol-1-yl]-1,3-thiazole-4(5H)-one : IR and FT-Raman bands and assignments

S. No	FTIR	FT-Raman	Calculated wavenumbers (cm^{-1})		Vibrational Assignment (%PED)
			Cam-B3LYP/6-31G (d,p)	B3LYP/6-311G (d,p)	
1	3061 vw	3065 ms	3071	3064	νCH (98)
2			3063	3059	νCH (97)
3			3058	3054	νCH (98)
4			3054	3051	νCH (98)
5			3049	3047	νCH (97)
6			3046	3042	νCH (98)
7			3039	3038	νCH (98)
8			3027	3021	νCH (97)
9			3019	3012	νCH (98)
10			3008	3003	νCH (96)
11			2999	2997	νCH (96)
12			2992	2988	νCH (97)
13			2988	2980	νCH (99)
14			2976	2972	νCH (98)
15			2968	2965	ν_{ass} CH_3 (89)
16			2957	2953	ν_{ass} CH_2 (88)
17			2946	2941	ν_{ass} CH_3 (88)
18			2934	2930	ν_{ass} CH_3 (88)
19			2925	2922	ν_{ass} CH_3 (88)
20			2917	2913	ν_{ss} CH_2 (89)
21			2909	2904	ν_{ss} CH_3 (88)
22			2895	2893	ν_{ss} CH_3 (90)
23			2889	2888	ν CH (95)
24	1668 m		1669	1667	νC=O (85)
25		1609 s	1611	1610	νCC (79), δCH (18)
26	1598 m	1596 vs	1599	1598	ν CN (76), νCC (18)
27			1578	1575	ν CC (72), δCH (27)
28			1567	1566	νCC (80), ν CN (12)
29		1562 vs	1562	1560	νCC (81), δCH (13)
30	1541 s		1543	1540	ν CC (68), δCH (22), δCC (10)
31			1526	1522	ν CC (65), δCH (18)
32			1510	1507	ν CN (89)
33	1489 s		1488	1486	ν CC (71), δCH (22)
34			1465	1461	δ CH (78)

Annals of R.S.C.B., ISSN:1583-6258, Vol. 25, Issue 3, 2021, Pages. 5674 - 5708
Received 16 February 2021; Accepted 08 March 2021.

35			1452	1448	δCH (78)
36			1441	1439	δCH (75)
37			1427	1422	$\delta_{ipb}CH_3$ (68)
38	1397 s	1401 s	1402	1400	$\delta_{ipb}CH_3$ (66)
39			1394	1391	$\delta_{opb}CH_3$ (67)
40			1387	1384	$\delta_{opb}CH_3$ (68)
41			1364	1362	$\delta_{siss}CH_2$ (71)
42			1355	1353	δCH (70)
43			1343	1341	δCH (72)
44			1332	1330	δCH (75)
45			1323	1318	δCH (75)
46			1315	1311	δ_{sym} CH_3 (72)
47	1327 s	1333 s	1309	1304	δCH (68)
48			1299	1297	δ_{sym} CH_3 (74)
49			1294	1290	δCH (77)
50		1285 s	1287	1284	δCH (75)
51	1274 ms		1278	1275	νCC (63)
52			1272	1269	νCC (62), δCH (12)
53			1265	1263	δCH (70), νCC (13)
54			1260	1258	δCH (71), νCC (12)
55		1250 vs	1251	1250	δCH (71), νCC (10)
56			1235	1234	νCC (68), δCH (17)
57	1225 w		1228	1225	νCC (67), δCCl (12), νCC (10)
58			1219	1214	δCH (69)
59			1207	1202	νCC (70), δCC (17), δCH (10)
60			1197	1195	δ_{rock} CH_2 (68), δCH (12)
61			1189	1188	νCC (68)
62	1183 ms	1182 s	1183	1180	νCC (68), δCH (12)
63			1174	1171	νCC (68), δCH (12)
64			1165	1163	δCH (66)
65			1153	1150	δCH (68)
66			1146	1141	νCN (63)
67			1132	1129	δCH (72)
68		1123 vs	1125	1120	τCH_2 (68)
69	1115 w		1118	1114	νCC (67)
70			1107	1105	δCH (70)
71			1098	1095	δCH (71)
72	1087 m	1089 m	1091	1088	δCH (70)
73			1072	1069	νNN (55), νCN (28)
74			1056	1054	$\delta_{ipr}CH_3$ (62)
75			1037	1033	νCCl (66), δCH (12)

Annals of R.S.C.B., ISSN:1583-6258, Vol. 25, Issue 3, 2021, Pages. 5674 - 5708
Received 16 February 2021; Accepted 08 March 2021.

76	1010 m		1015	1011	νCCl (68), δCH (12)
77			999	998	$\delta_{ipr}CH_3$ (60)
78			994	991	δCC (61)
79			989	988	δCC (60), δCH (13)
80			985	982	δCC (62), δCH (12)
81			978	973	δCC (62), δCH (12)
82			967	963	δCC (66), δCN (16)
83	952 w	950 m	954	951	γCH (59)
84			945	941	γCH (60)
85			939	934	νSC (70), δCH (16), νCC (10)
86			931	928	γCH (60)
87			919	917	γCH (61)
88			905	902	γCH (58)
89	897 m		899	895	γCH (58)
90			890	888	$\gamma_{opr}CH_3$ (60)
91			875	870	γCH (58)
92			857	855	νCN (58), νCC (27)
93			844	840	$\gamma_{opr}CH_3$ (58)
94			835	832	γCH (60)
95	825 s	823 w	827	825	νCC (68)
96			819	814	γCH (76)
97			810	809	γCH (68)
98			808	804	γCH (66)
99			797	795	γCH (68)
100			789	788	γCH (56)
101			769	767	γCH (65)
102			762	759	γCH (66)
103	747 m	748 w	753	750	γCH (65)
104			745	740	γCH (65)
105			734	731	δ_{ring} (58)
106			726	720	δ_{ring} (58)
107		711 w	719	712	γCO (62), γCH (12)
108	706 ms		710	705	γ_{ring} (57)
109			687	681	δ_{ring} (60)
110			672	668	γ_{ring} (55)
111			648	643	γ_{ring} (55)
112			624	619	γ_{ring} (58)
113			597	594	γ_{ring} (60)
114	589 w		592	588	δCC (62)
115			579	575	δ_{ring} (66)
116			572	570	δ_{ring} (66)

Annals of R.S.C.B., ISSN:1583-6258, Vol. 25, Issue 3, 2021, Pages. 5674 - 5708
Received 16 February 2021; Accepted 08 March 2021.

117			567	563	δ_{ring} (65)
118		554 w	559	555	δ_{ring} (66)
119			541	538	γ_{ring} (55)
120			495	491	γ_{ring} (55)
121	501 w		478	475	νCS (62)
122			469	467	νCS (63), δCO (16)
123	461 w		465	460	σ_{wagg} CH_2 (62)
124			448	444	γ_{ring} (60)
125			441	439	γ_{ring} (60)
126	436 vw		426	422	δ_{ring} (61)
127			407	403	δCC (57)
128			398	394	δCC (58)
129			389	386	ν CCl (63)
130			377	375	ν CCl (62)
131			371	369	γ_{ring} (58)
132			356	353	γ_{ring} (55)
133			335	332	γ_{ring} (54)
134			326	320	γCC (52)
135			308	304	γCC (50)
136			296	292	γCH (53)
137			285	281	γCC (52)
138			278	275	γCC (52)
139			272	269	γCC (52), γCCl (18)
140			265	260	δ_{ring} (62)
141			257	253	δCCl (62)
142			246	241	δCCl (64)
143			235	230	γCC (52)
144			219	217	γCC (52)
145			208	203	γCC (52)
146			199	197	τCH_3 (52)
147			192	189	τCH_3 (52)
148			184	179	γCC (53)
149			176	170	δCC (60)
150			163	159	γCCl (53)
151			154	148	γCCl (50)
152			141	137	γ_{ring} (48)
153			117	112	γ_{ring} (50)
154			109	103	γ_{ring} (52)
155			97	91	δ_{ring} (56)
156		81 m	86	80	γCC (52)
157			78	74	δCC (55)

Annals of R.S.C.B., ISSN:1583-6258, Vol. 25, Issue 3, 2021, Pages. 5674 - 5708
Received 16 February 2021; Accepted 08 March 2021.

158			73	71	δCC (56)
159			69	68	τCC (49)
160			56	50	τCC (50)
161			47	45	τCC (50)
162			36	31	τCC (48)
163			31	28	τCC (50)
164			27	25	τCC (48)
165			24	21	τCC (48)
166			21	20	τCC (48)
167			19	16	τCC (48)
168			10	8	τCC (50)

Abbreviations: ν: stretching, δ: in-plane bending, γ: out-of-plane bending, ass: asymmetric stretching, ss: symmetric stretching, τ: torsion, siss – scissoring, wag: wagging.

C-S vibration

The C-S stretching vibration mode can be found in an extensive range 1035-245 cm^{-1} in both aliphatic and aromatic sulfides, since it is absorbed as strong bands in Raman spectra are normally easy to identify [33,50]. In this study, non-polar covalent C-S stretching vibration assigned at 939, 934 cm^{-1} (70%) and at 501cm^{-1} observed in FT-Raman spectrum, 478, 475, 469, 467 cm^{-1} (62%) obtained theoretically by CAM-B3LYP/6-31G (d,p) and B3LYP/6-311G (d,p) methods. The reported C-S stretching vibrations were assigned at 646, 639 cm^{-1} [51], 752 cm^{-1} [52] theoretically and at 820,658 cm^{-1}(IR) [53]. Viji et al.[12] reported the C-S stretching vibration at 664 cm^{-1} in IR spectrum, 658 cm^{-1} in FT-Raman spectrum, 660, 662, 655, 654 cm^{-1} theoretically and at 854 cm^{-1} in IR spectra, theoretically computed at 860, 854, 786, 785 cm^{-1} given by venil et al.[46].

C-N, N-N vibrations

According to the survey of the C-N stretching vibration mode obtained in the range of 1600-1100 cm^{-1} of pyrazole ring at variable intensities. In general, these vibration modes were assigned in the range 1300-1100 cm^{-1} [27, 35], so these vibration modes are very difficult job to identify. The C=N stretching vibration mode was observed at 1600 cm^{-1} in FT-IR spectrum by V.V.Salian et al.[16]. P. Rajamani et al.[54] reported experimentally observed at 1588 cm^{-1} and 1571 cm^{-1} in FT-IR and Raman spectra respectively and at 1488, 1383, 1333, 998 cm^{-1} calculated by Y. Sert et al.[55]. The reported C-N stretching vibration modes were assigned at 1491, 1332 cm^{-1} in IR spectrum, 1530, 1493,1485,1336 cm^{-1} theoretically by venil et al.[46], at 1546

Annals of R.S.C.B., ISSN:1583-6258, Vol. 25, Issue 3, 2021, Pages. 5674 - 5708
Received 16 February 2021; Accepted 08 March 2021.

cm^{-1}(IR), 1549 cm^{-1} (Ra) and calculated bands obtained at 1625, 1551,1525, 1205, 1106, 1025 cm^{-1} for C-N stretching and at 963, 960 cm^{-1} assigned to C-N in-plane bending mode by Sivakumar et al.[15]. In the studied molecular structure, the C-N bands were accomplished at 1598 cm^{-1} and 1596 cm^{-1} in FT-IR and FT-Raman spectra refer to stretching vibration mode. The calculated values are found at 1599, 1510, 1146, 857 cm^{-1} and 1598, 1507, 1141, 857 cm^{-1} with PED contribution of 76, 89, 63, 58% by CAM-B3LYP/6-31G (d,p) and B3LYP/6-311G(d,p) methods. The band at 963 and 967 cm^{-1} are associated to C-N in-plane bending vibration of the title molecule. These assigned wavenumbers had a better correlation with those reported in literature survey.

The N-N stretching vibration mode of the pyrazole ring is expected in the range of 1100-950 cm^{-1} [39]. This vibration mode is assigned at 1072, 1069 cm^{-1} for studied molecular structure theoretically. For the similar pyrazole ring N-N vibration mode reported at 894 cm^{-1} for PHOXPY, 917cm^{-1} for STOXPY and at 926cm^{-1} for FUOXPY theoretically by A.S.El-Azab et al.[56]. M.Sathish et al.[39] reported at 1135cm^{-1} in FT-Raman spectrum and calculated at 1132cm^{-1} for N-N vibration mode belonging pyrazole ring. Al-Tamimi et al.[36] reported that computed values of N-N vibration has 944, 921, 895 cm^{-1} and these values are in good agreement with literature.

3.3 **Molecular electrostatic potential**

The molecular electrostatic potential for the title compound has been shown in Figure 4 in the range of -6.590e-2 a.u to 6.590e-2 a.u at B3LYP/6-311G (d,p) basis set. It provides various information about the molecular activities such as electrophilicity, nucleophilicity, hydrogen bonding, hydronation/dehydronation and distinct other desirable molecular interactions. Bright red colored surface describes the relative abundance of electrons that indicate negative potential surface of the molecule viz., C and O atom (V(r) < -6.590e-2 a.u). Pyrazole ring N-atoms has comparatively less negative potential than that of O-atom. Since, its lone pair of electrons involved in an aromatic delocalization and S-atom seems to be concealed inside the highest possible positive potential surface of the studied compound.

Annals of R.S.C.B., ISSN:1583-6258, Vol. 25, Issue 3, 2021, Pages. 5674 - 5708
Received 16 February 2021; Accepted 08 March 2021.

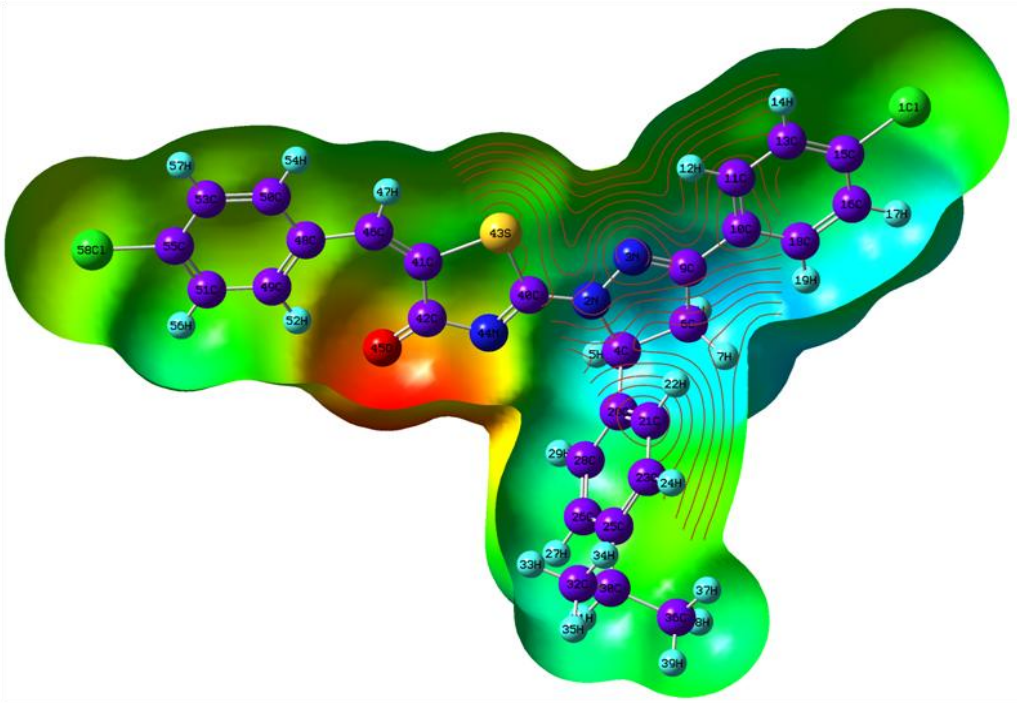

Figure 4. Molecular electrostatic potential of 5-(4-Chlorobenzylidene)-2-[3-(4-chlorophenyl)-5-[4-(propan-2-yl) phenyl]-4-5-dihydro-1*H*-pyrazol-1-yl]-1, 3-thiazole-4(5*H*)-one

3.4 Frontier molecular orbital

After geometric optimization the highest occupied molecular orbital (HOMO) and lowest unoccupied orbital (LUMO) criterions are very influential to find out quantum chemistry mechanism and chemical reactivity. Generally energy is related to ionization potential known as donor, although LUMO energy is related to electron activation as acceptor. And the energy differences between HOMO and LUMO called energy gap ($\Delta E = E_{LUMO} - E_{HOMO}$) plays crucial role to determined stability of the molecule. While the energy gap of the molecule have been small represents low kinetic stability. It results the significant degree of intermolecular charge transfer from HOMO to LUMO through π- conjugated path. The following parameters were computed from HOMO to LUMO energy values as; Ionization potential: $I = -E_{HOMO}$, Electron affinity: $A = -E_{LUMO}$, Chemical hardness: $\eta = \frac{(I - A)}{2}$, Electron chemical potential: $\mu = \frac{1}{2}(E_{LUMO} + E_{HOMO})$, Eleectrophilicity index: $\psi = \frac{\mu^2}{2\eta}$,

Annals of R.S.C.B., ISSN:1583-6258, Vol. 25, Issue 3, 2021, Pages. 5674 - 5708
Received 16 February 2021; Accepted 08 March 2021.

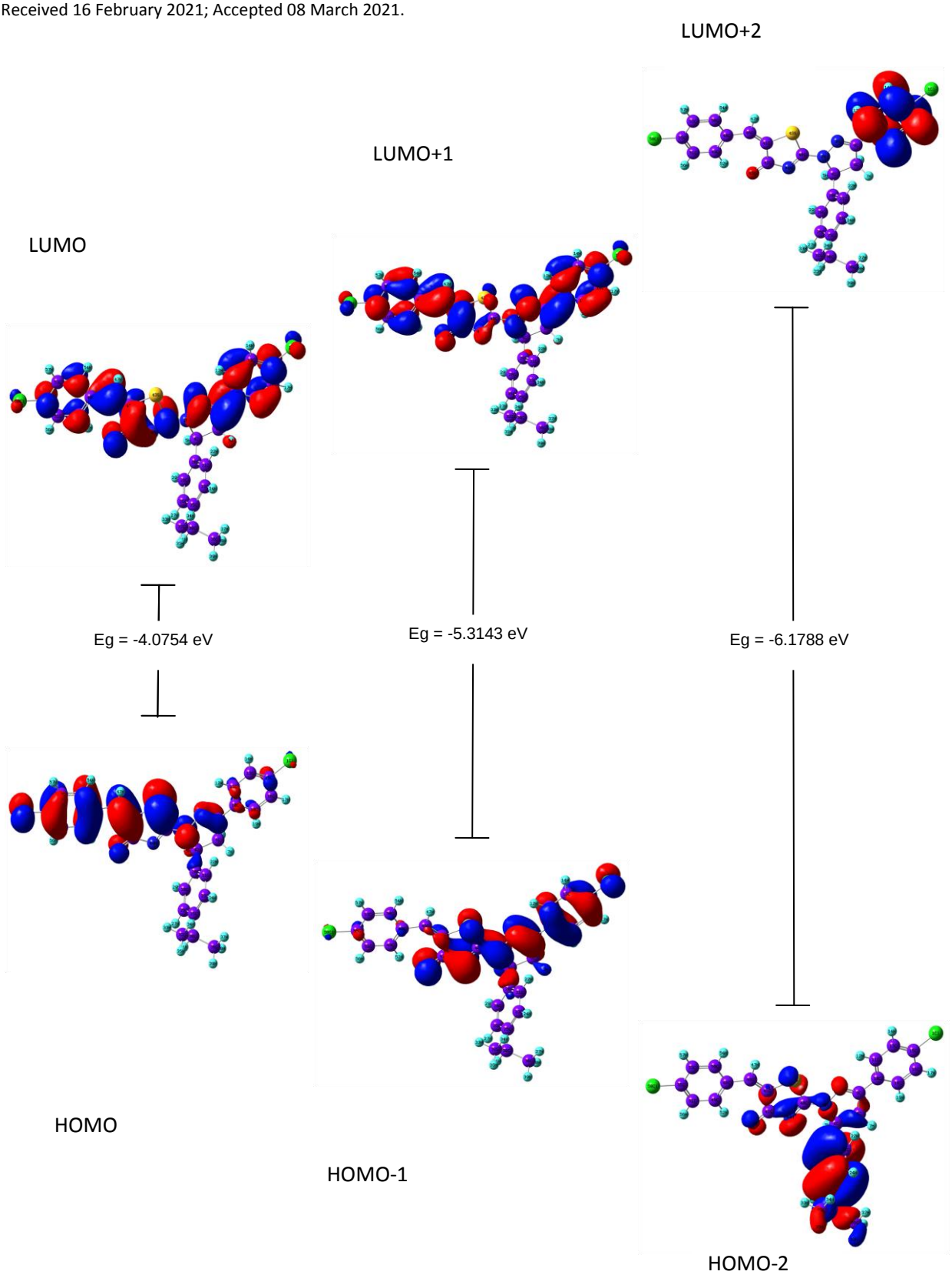

Figure 5. Frontier molecular orbital of 5-(4-Chlorobenzylidene)-2-[3-(4-chlorophenyl)-5-[4-(propan-2-yl) phenyl]-4-5-dihydro-1*H*-pyrazol-1-yl]-1, 3-thiazole-4(5*H*)-one

Annals of R.S.C.B., ISSN:1583-6258, Vol. 25, Issue 3, 2021, Pages. 5674 - 5708
Received 16 February 2021; Accepted 08 March 2021.

Softness: $\zeta = \frac{1}{2\eta}$ [57-59] tabulated in Table 3. Figure 5 shows the distribution of HOMO-LUMO cloud stimulated from the optimized molecular geometry computed in gas phase at B3LYP/6-311G (d,p) level for the tested compound. In the present molecule E_{LUMO} = -1.9437 eV, E_{HOMO} = -6.0191 eV, energy gap E_g = -4.0754 eV, global hardness η = 2.0377 eV, chemical potential μ= -3.9814 eV, and global electrophilicity =3.8895 eV. When the chemical potential of the investigated compound seems to be negative, it refers to higher kinetic stability of the studied compound.

Table 3: Calculated HOMO-LUMO energy gap and Global reactive descriptors of 5-(4-Chlorobenzylidene)-2-[3-(4-Chlorophenyl)-5-[4-(propan-2-yl) phenyl]-4-5-dihydro-1H-pyrazol-1-yl]-1,3-thiazole-4(5H)-one using B3LYP/6-311G(d,p) basis set

State	Energy gap (a.u)	Energy gap (eV)	Hardness (eV)	Softness (eV)	Electrophilicity (eV)	Electronegativity (eV)
HOMO	0.1497	-4.0754	2.0377	0.2454	3.8895	3.9814
LUMO						
HOMO-1	0.1953	-5.3143	2.6572	0.1882	2.6815	3.7750
LUMO+1						
HOMO-2	0.2270	-6.1788	3.0894	0.1618	2.3118	3.7795
LUMO+2						

3.5 Natural bond analysis

The knowledge of interactions between donor and acceptor of the molecular structure in the natural bond orbital analysis were elucidated with the help of second order perturbation theory [60, 61]. The highest possible electron density distribution of the molecule among the orbital were given by NBO analysis. The equation related for the stabilization energy $E^{(2)}$ were given by

$$E^{(2)} = q_i \frac{F_{ij}^{\ 2}}{\varepsilon_j - \varepsilon_i}$$

Annals of R.S.C.B., ISSN:1583-6258, Vol. 25, Issue 3, 2021, Pages. 5674 - 5708
Received 16 February 2021; Accepted 08 March 2021.

Where, the off-diagonal components are represented as ε_j and ε_i. F_{ij} is the diagonal and E^2 measured in kcal/mol by NBO Fock matrix elements. Also q_i deliberates from the donor orbital occupancy. For the studied compound of natural bond analysis investigation is an impressive tool

Table 4: Second order perturbation theory analysis corresponding to intra- molecular bands of 5-(4-Chlorobenzylidene)-2-[3-(4-Chlorophenyl)-5-[4-(propan-2-yl) phenyl]-4-5-dihydro-1H-pyrazol-1-yl]-1,3-thiazole-4(5H)-one by B3LYP/6-311G (d, p) basis set in NBO.

S. No	Type	Donor (i)	ED/e	Typ	Acceptor (j)	ED/e	E(2) kcal/mol	E(j)-E(i) a.u.	F(i,j) a.u.
1	σ	N2 - N3	1.98075	σ*	C9 - C10	0.03388	4.85	1.32	0.072
2	σ	N3 - C9	1.98396	σ*	N2 - C40	0.06393	4.69	1.2	0.068
3	π	N3 - C9	1.91092	π*	C10 - C18	0.38066	9.04	0.37	0.055
4	π	C10 - C18	1.64605	π*	N3 - C9	0.23861	18.88	0.28	0.067
5	π	C10 - C18	1.64605	π*	C11 - C13	0.28502	18.5	0.29	0.067
6	π	C10 - C18	1.64605	π*	C15 - C16	0.38619	20.95	0.28	0.068
7	σ	C11 - C13	1.96634	σ*	Cl 1 - C15	0.03467	5.6	0.84	0.061
8	π	C11 - C13	1.67932	π*	C10 - C18	0.38066	19.2	0.29	0.067
9	π	C11 - C13	1.67932	π*	C15 - C16	0.38619	22.06	0.27	0.071
10	π	C15 - C16	1.68717	π*	C10 - C18	0.38066	18.17	0.3	0.067
11	π	C15 - C16	1.68717	π*	C11 - C13	0.28502	18.6	0.31	0.068
12	σ	C16 - C18	1.96526	σ*	Cl 1 - C15	0.03467	5.76	0.84	0.062
13	π	C20 - C28	1.65682	σ*	N2 - C4	0.06379	5.8	0.55	0.054
14	π	C20 - C28	1.65682	π*	C21 - C23	0.32692	20.99	0.28	0.069
15	π	C20 - C28	1.65682	π*	C25 - C26	0.33838	19.35	0.29	0.067
16	π	C21 - C23	1.67414	π*	C20 - C28	0.35676	19.97	0.29	0.068
17	π	C21 -	1.6741	π*	C25 - C26	0.3383	21.44	0.29	0.07

Annals of R.S.C.B., ISSN:1583-6258, Vol. 25, Issue 3, 2021, Pages. 5674 - 5708
Received 16 February 2021; Accepted 08 March 2021.

		C23	4			8			1
18	π	C25 - C26	1.63922	π*	C20 - C28	0.35676	23.1	0.28	0.072
19	π	C25 - C26	1.63922	π*	C21 - C23	0.32692	20.05	0.28	0.067
20	σ	C40 - S43	1.97765	σ*	C41 - C46	0.03566	7.29	1.21	0.084
21	σ	C40 - N44	1.96445	σ*	C42 - O45	0.06953	6.09	1	0.07
22	σ	C41 - C42	1.97847	σ*	C41 - C46	0.03566	4.52	1.02	0.061
23	σ	C41 - S43	1.97963	σ*	C41 - C46	0.03566	4.7	1.37	0.072
24	σ	C49 - C51	1.96810	σ*	C46 - C48	0.03014	4.72	1.05	0.063
25	σ	C50 - H54	1.97307	σ*	C48 - C49	0.05308	4.64	1.09	0.064
26	σ	C51 - H56	1.97103	σ*	C53 - C55	0.02919	4.68	1.09	0.064
27	σ	C53 - H57	1.97638	σ*	C51 - C55	0.04573	4.64	1.09	0.064
28	LP(2)	Cl 1	1.97009	σ*	C13 - C15	0.03044	4.68	0.89	0.058
29	LP(2)	Cl 1	1.97009	σ*	C15 - C16	0.02986	4.58	0.9	0.057
30	LP(3)	Cl 1	1.92451	π*	C15 - C16	0.38619	13.2	0.33	0.064
31	LP(1)	N2	1.69040	π*	N3 - C9	0.23861	26.31	0.28	0.079
32	LP(1)	N2	1.69040	σ*	C40 - N44	0.10786	6.62	0.56	0.059
33	LP(1)	N3	1.93019	σ*	N2 - C4	0.06379	8.1	0.72	0.068
34	LP(1)	N3	1.93019	σ*	C6 - C9	0.03554	8.12	0.8	0.073
35	LP(1)	S43	1.93775	σ*	C41 - C42	0.07059	8.94	0.94	0.083
36	LP(1)	S43	1.93775	σ*	C42 - O45	0.06953	0.55	0.85	0.019
37	LP(1)	N44	1.93078	σ*	C41 - C42	0.07059	6.55	0.8	0.065
38	LP(2)	O45	1.86153	σ*	C41 - C42	0.07059	9.56	0.63	0.07
39	LP(2)	O45	1.86153	σ*	C42 - N44	0.01684	11.74	0.69	0.081

Annals of R.S.C.B., ISSN:1583-6258, Vol. 25, Issue 3, 2021, Pages. 5674 - 5708
Received 16 February 2021; Accepted 08 March 2021.

40	π*	C15 - C16	0.38619	π*	C10 - C18	0.38066	294.94	0.01	0.084
41	π*	C15 - C16	0.38619	π*	C11 - C13	0.28502	225.16	0.01	0.081

for expose intra and inter molecular bonding and also evaluate conjugative interactions in the molecular structure. The electron devoting shift from donors to acceptors in any molecular system may lended larger values of the E^2. The summarized NBO data of the molecular structure were tabulated in Table 4. The immense stabilized energies of the strong $\pi - \pi^*$ conjugative interactions were π (C11-C13) $\rightarrow \pi^*$(C15-C16), π (C21-C23) $\rightarrow \pi^*$(C25-C26), π (C10-C18) $\rightarrow \pi^*$(C15-C16), π (C20-C28) $\rightarrow \pi^*$(C21-C23) and π (C25-C26) $\rightarrow \pi^*$(C21-C23) with energy value of 22.06, 21.44, 20.95, 20.99 and 20.05 kcal/mol respectively. Also the minimum stabilization energy of the transition having π (N3-C9) $\rightarrow \pi^*$(C10-C18) contains 9.04kcal/mol.

Based on the weak donor (σ) $\rightarrow$ (σ^*) interactions due to $\sigma \rightarrow \sigma^*$ transitions were studied for the title compound resulting in least stabilization energy values $E^{(2)}$. σ (C40-S43) $\rightarrow \sigma^*$(C41-C46) with $E^{(2)}$ value 7.29 kcal/mol showing higher value amongst all $\sigma \rightarrow \sigma^*$ transitions and σ (C41-C42) $\rightarrow \sigma^*$(C41-C46) having 4.52 kcal/mol shows least energy value. The interaction of electron delocalization of the compound occurs between π^*(C15-C16) $\rightarrow \pi^*$(C10-C18) and π^*(C15-C16) $\rightarrow \pi^*$(C11-C13) with large value of stabilization energy as 294.94 and 225.16 kcal/mol respectively which could be the impulse for bioactive behavior of the molecule [62]. The lone pair making anti bonding interaction with higher stabilization energies are LP3 (Cl1) $\rightarrow \pi^*$(C15-C16) and LP1(N2) $\rightarrow \pi^*$(N3-C9) having $E^{(2)}$ value 13.2 and 26.31 kcal/mol. While LP2(O45) $\rightarrow \sigma^*$(C42-N44), LP2(O45) $\rightarrow \sigma^*$(C41-C42), LP1(S43) $\rightarrow \sigma^*$(C41-C42), LP1(N3) $\rightarrow \sigma^*$(C6-C9), LP1(N3) $\rightarrow \sigma^*$(N2-C4) and LP1(N2) $\rightarrow \sigma^*$(C40-N44) produced 11.74, 9.56, 8.94, 8.12, 8.10 and 6.62 kcal/mol which shows least electron donating interaction energies in the studied molecular structure correspondingly.

3.6 ***Biological application: Docking studies***

The molecular docking analysis of different protein in anti-tumor, antifungal and antibacterial activity of the title compound was carried out by using Auto Dock software and Discover studio visualizer 4.1 software [23, 24]. Docking of the subjected molecular compound

Annals of R.S.C.B., ISSN:1583-6258, Vol. 25, Issue 3, 2021, Pages. 5674 - 5708
Received 16 February 2021; Accepted 08 March 2021.

into the binding site of a receptor and supposing the binding affinity is an influential part of the drug design process. A complete molecular view and a graphical support computationally offered by Auto Dock Tools for all steps required for run docking process. The X-ray crystal structures of the selected protein were downloaded from the RSCB protein data bank website (PDB ID: 1DLG, 1NQ3, 2KCN, 3A7I, 4OQS, 5W7M, 3BCI, 3T8R) [63]. The rigid docking process was carried out in the form of macromolecule active sites within grid box size of 60Åx60Åx60Å (spacing = 0.375Å) over the target protein binding pocket. About 100 genetic algorithm runs, the minimum binding affinity values were obtained to anti-tumor (PDB ID: 1DLG, 1NQ3/-8.90, -8.89 kcal/mol), antifungal (PDB ID: 2KCN, 3A7I, 4OQS, 5W7M/-7.05, -9.58, -7.75, -8.53 kcal/mol) and antibacterial (PDB ID: 3BCI, 3T8R/-8.39, -6.30 kcal/mol)

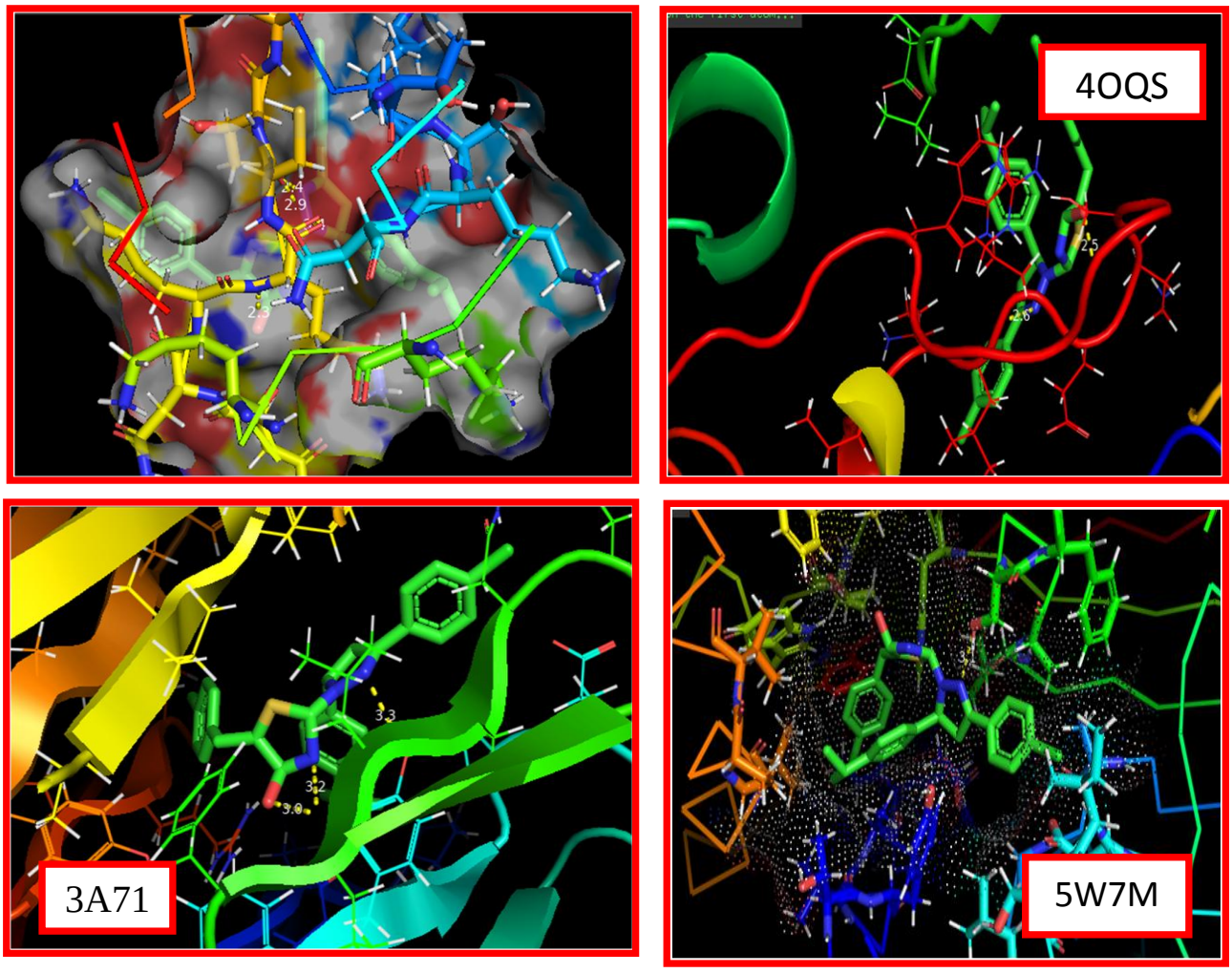

Figure 6. Molecular docking of 5-(4-Chlorobenzylidene)-2-[3-(4-chlorophenyl)-5-[4-(propan-2-yl) phenyl]-4-5-dihydro-1*H*-pyrazol-1-yl]-1, 3-thiazole-4(5*H*)-one

Annals of R.S.C.B., ISSN:1583-6258, Vol. 25, Issue 3, 2021, Pages. 5674 - 5708
Received 16 February 2021; Accepted 08 March 2021.

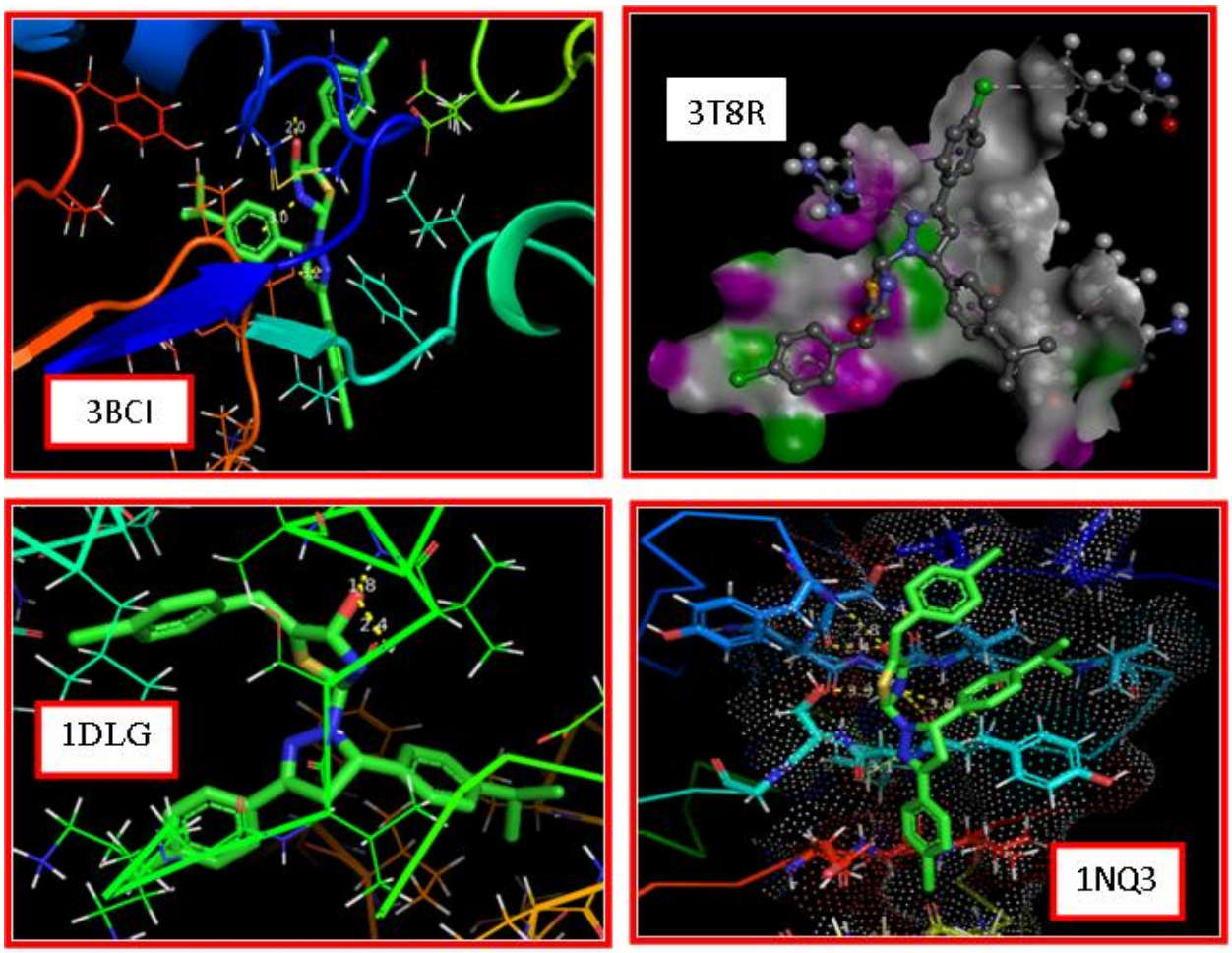

Figure 7 Molecular docking of 5-(4-Chlorobenzylidene)-2-[3-(4-chlorophenyl)-5-[4-(propan-2-yl) phenyl]-4-5-dihydro-1*H*-pyrazol-1-yl]-1, 3-thiazole-4(5*H*)-one

proteins might be beneficial for biological activity with title compound. The lowest value of inhibition constant was an essential parameter desired in molecular docking studies, which is obtained in Table 5. The binding distance of anti-tumor protein were obtained as 1.84Å (GLY A: 162), 3.56Å (Alkyl), 3.40Å (ILE A: 327) in 1DLG and the oxygen and nitrogen atoms bind with 1NQ3 protein of distance 3.03Å (ALA A: 24) and 3.05Å (TRY A:32), 2.17Å (SER A:22). The ligand- protein interaction between antifungal protein shows carbon-hydrogen interaction with 2.82Å (ASP A: 32) in 2KCN and π-Lone pair interaction of 2.83Å (ALA A: 179), H-bond at 2.97Å (LEU A: 177; O), 3.22Å (LEU A: 177;N) in 3A7I protein. The distance for H-bond, carbon–hydrogen and π-donor hydrogen bond interactions were obtained as 2.60Å (SER A: 387; O), 2.70Å (GLU A: 385;N), 2.66Å (ARG A: 384;N) and 2.71Å (LEU A: 383) in 4OQS.

Annals of R.S.C.B., ISSN:1583-6258, Vol. 25, Issue 3, 2021, Pages. 5674 - 5708
Received 16 February 2021; Accepted 08 March 2021.

The H-bond interaction of 'N' atom is at 2.25Å (SER A: 131), sulfur-X interaction at 3.23Å (TRP A: 157) and alkyl interaction recorded at 3.64Å (ALA A: 54), 3.44Å (ALA A: 23) is formed with chlorophenyl ring of ligand in 5W7M. There are H-bond interactions of =O at 2.01Å (TYR A: 28), 3.01Å (CYS A: 26), 2.98Å (CYS A: 26; N), 3.0Å (THR A: 153) and π-lone pair interaction formed at 2.89Å (LYS: 151) of antibacterial protein in 3BCI. The π-donor hydrogen interaction formed at 2.47Å (ASN A: 35), π-sigma and H-bond were obtained at 2.85Å (ARG A: 8) and 2.15Å (ARG A: 8; N) in 3T8R protein. Figure 6 and 7 showed the details about the binding interaction of the receptor with the title compound.

Table 5: Molecular binding affinity for docking in 5-(4-Chlorobenzylidene)-2-[3-(4-chlorophenyl)-5-[4-(propan-2-yl) phenyl]-4-5-dihydro-1H-pyrazol-1-yl]-1,3-thiazole-4(5H)-one

Protein Name	Pub Chem ID	Amino acid	Bond Interaction	Bond Length (Å)	**Binding Energy (kcal/mol)**	**Inhibition Constant (molar)**
E.Coli Cancer	1DLG	GLY A:164	Conventional Hydrogen	1.84	-8.90	299.82 nM
		SER A:162	Carbon Hydrogen	3.40		
		ILE A:327	Alkyl Interaction	3.56		
Tumor	1NQ3	SER A:22	Carbon Hydrogen	2.17	-8.89	305.36 nM
		SER A:22	Conventional Hydrogen	2.40		
		SER A:22	Conventional Hydrogen	2.79		
		ALA A:24	Carbon Hydrogen	3.03		
		TRY A:32	Conventional Hydrogen	3.05		
S. Auraus	3BCI	TYR A:28	Conventional Hydrogen	2.01	-8.39	711.70 nM
		LYS A:151	Pi-Lone pair	2.89		
		CYS A:26	Conventional Hydrogen	2.98		
		THR A:153	Conventional Hydrogen	3.00		

Annals of R.S.C.B., ISSN:1583-6258, Vol. 25, Issue 3, 2021, Pages. 5674 - 5708
Received 16 February 2021; Accepted 08 March 2021.

		CYS A:26	Conventional Hydrogen	3.01		
	3T8R	ARG A:8	Conventional Hydrogen	2.15	-6.30	23.97 μM
		ASN A:35	Pi-Donor Hydrogen	2.47		
		ARG A:8	Pi-Sigma	2.85		
Penicillium	2KCN	ASP A:32	Carbon Hydrogen	2.82	-7.05	6.79 μM
	3A71	ALA A:179	Pi-Lone pair	2.83	-9.58	94.60 nM
		LEU A:177	Conventional Hydrogen	2.97		
		LEU A:177	Conventional Hydrogen	3.22		
	4OQS	SER A:387	Conventional Hydrogen	2.60	-7.75	2.08 μM
		ARG A:384	Carbon-Hydrogen	2.66		
		GLU A:385	Conventional Hydrogen	2.70		
		LEU A:383	Pi-Donor Hydrogen	2.71		
	5W7M	SER A:131	Conventional Hydrogen	2.25	-8.53	557.42 nM
		TRP A:157	Sulfur-x interaction	3.23		
		ALA A:23	Alkyl	3.44		
		ALA A:54	Alkyl	3.64		

4. Conclusion

In present study, the optimized structure of studied molecule compared with X-ray crystallographic data of related molecule was found to be reliable agreement. The stimulated vibrational spectrums of present molecule have been obtained from density functional theory

(DFT) method of different level exhibits good agreement with experimental one while compared in solid phase. The HOMO – LUMO energy gap has evident that there is a significant influence on bioactivity of the molecule. The reactive site of the molecule has been located by MEP study. The ligand forms a stable complex with the proteins and gives good binding affinities and the preliminary docking results suggest that the title compound exhibits inhibitory activity against *S. aureus*, E. coli-anti-cancer and Pencillium. This could be useful to develop a new drug.

Reference:

[1] O. S¸ ahin, Ü.€O. €Ozdemir, N. Sefero_glu, Z.K. Genc, K. Kaya, B. Aydıner, S. Tekin, Z. Sefero_glu, J. Photochem. Photobiol. B Biol. 178 (2018) 428-439.

[2] G.M. Ziarani, R. Moradi, T. Ahmadi, N. Lashgari, RSC Adv. 8 (2018) 12069-12103.

[3] B.Z. Kurt, I. Gazioglu, F. Sonmez, M. Kucukislamoglu, Bioorg. Chem. 59 (2015) 80 - 90.

[4] Z. Jin, Muscarine, imidazole, oxazole and thiazolee alkaloids, Nat. Prod. Rep. 28 (2011) 1143-1191.

[5] H.Y. Jiang, C.H. Zhou, K. Luo, H. Chen, J.B. Lan, R.G. Xie, Chiral imidazole metallo enzyme models, Synthesis and enantioselective hydrolysis for a-amino acid esters, J. Mol. Catal. Chem. 260 (2006) 288-294.

[6] M. Maeda, Laser Dyes, Academic, New York, 1994.

[7] B.S. Creaven, B. Duff, D.A. Egan, Inorg. Chim. Acta 363 (2010) 4048-4058.

[8] Iqbal Azad, Asif Jafri, Tahmeena Khan, Yusuf Akhter, Md Arshad, Firoj Hassan, Naseem Ahmad, Abdul Rahman Khan, Malik Nasibullah, " Evaluation of pyrrole-2,3-dicarboxylate derivatives: Synthesis, DFT analysis, molecular docking, virtual screening and in vitro anti-hepatic cancer study" Journal of Molecular Structure 1176 (2019) 314-334.

[9] U. Asghar, T. Meyer, Are there opportunities for chemotherapy in the treatment of hepatocellular cancer? J. Hepatol. 56 (2012) 686-695, https://doi.org/10.1016/J.JHEP.2011.07.031 .

[10] J.H. Al-Fahemi, A.M. Khedr, I. Althagafi, N.M. El-Metwaly, F.A. Saad, H.A. Katouah, Appl. Organomet. Chem. 32 (9) (2018) e4460.

[11] Nashwa El-Metwaly, Ismail Althagafi, Abdalla M. Khedr, Jabir H. Al-Fahemi, Hanadi A. Katouah, Aisha S. Hossan, Aisha Y. Al-Dawood, Gamil A. Al-Hazmi, "Synthesis and characterization for novel Cu(II)-thiazolee complexes dyes and their usage in dyeing cotton

to be special bandage for cancerous wounds" Journal of Molecular Structure 1194 (2019) 86-103.

[12] A.Viji, V.Balachandran, S.Babiyana, B.Narayana, Vinutha V.Saliyan, Molecular docking and quantum chemical calculations of 4-methoxy-{2-[3-(4-chlorophenyl)-5-(4-(propane-2-yl) phenyl)-4, 5-dihydro-1*H*-pyrazol-1-yl]- 1, 3-thiazole-4-yl}phenol, Journal of Molecular Structure Volume 1203, 5 March 2020, 127452.

[13] C.Sivakumar, V.Balachandran, B.Narayana, VinuthaV.Salian, B.Revathi, N.Shanmugapriya, K.Vanasundari, Molecular spectroscopic assembly of 3-(4-chlorophenyl)-5-[4-(propane-2-yl) phenyl] 4, 5-dihydro-1*H* pyrazole-1-carbothioamide, antimicrobial potential and molecular docking analysis, Journal of Molecular Structure Volume 1210, 15 June 2020, 128005.

[14] A.Viji, V.Balachandran, S.Babiyana, B.Narayana, Vinutha V.Salian, FT-IR and FT-Raman investigation, quantum chemical studies, molecular docking study and antimicrobial activity studies on novel bioactive drug of 1-(2,4-Dichlorobenzyl)-3-[2-(3-(4-chlorophenyl)-5-(4-(propan-2-yl)phenyl-4,5-dihydro-1H-pyrazol-1-yl]-4-oxo-4,5-dihydro-1,3-thiazole-5(4H)-ylidence]-2,3-dihydro-1H-indol-2-one, Journal of Molecular Structure Volume 1215, 5 September 2020, 128244.

[15] C Sivakumar, B Revathi, V Balachandran, B Narayana, Vinutha V Salian, N Shanmugapriya, K Vanasundari, Molecular structure, spectroscopic, quantum chemical, topological, molecular docking and antimicrobial activity of 3-(4-Chlorophenyl)-5-[4-propan-2-yl) phenyl-4, 5-dihydro-1H-pyrazol-1-yl](pyridin-4-yl) methanone, Journal of Molecular Structure Volume 1224, 15 January 2021, 129286.

[16] V.V. Salian, B. Narayana, B.K. Sarojini, M.S. Kumar, K. Sharath Chandra, A.G. Lobo, Tailor made biheterocyclic pyrazoline-thiazoleidinones as effective inhibitors of Escherichia coli FabH: Design, synthesis and structural studies, Journal of Molecular Structure 1192 (2019) 91-104.

[17] Gaussian 09, Revision B.01, M.J. Frisch, G.W. Trucks, H.B. Schlegel, G.E. Scuseria, M. A. Robb, J.R. Cheeseman, G. Scalmani, V. Barone, B. Mennucci, G.A. Petersson, H. Nakatsuji, M. Caricato, X. Li, H.P. Hratchian, A.F. Izmaylov, J. Bloino, G. Zheng, J.L. Sonnenberg, M. Hada, M. Ehara, K. Toyota, R. Fukuda, J. Hasegawa, M. Ishida, T. Nakajima, Y. Honda, O. Kitao, H. Nakai, T. Vreven, J.A. Montgomery, Jr., J.E. Peralta, F. Ogliaro, M. Bearpark, J.J.

Heyd, E. Brothers, K.N. Kudin, V.N. Staroverov, T. Keith, R. Kobayashi, J. Normand, K. Raghavachari, A. Rendell, J.C. Burant, S.S. Iyengar, J. Tomasi, M. Cossi, N. Rega, J.M. Millam, M. Klene, J.E. Knox, J.B. Cross, V. Bakken, C. Adamo, J. Jaramillo, R. Gomperts, R.E. Stratmann, O. Yazyev, A.J. Austin, R. Cammi, C. Pomelli, J.W. Ochterski, R.L. Martin, K. Morokuma, V.G. Zakrzewski, G.A. Voth, P. Salvador, J.J. Dannenberg, S. Dapprich, A.D. Daniels, O. Farkas, J.B. Foresman, J.V. Ortiz, J. Cioslowski, D.J. Fox, Gaussian, Inc., Wallingford CT, 2010.

[18] BENMEKHBI, L., et al. "INHIBITION STUDY BY MOLECULAR DOCKING OF DIHYDROFOLATE REDUCTASE OF ESCHERICHIA COLI WITH SOME CHALCONE MOLECULES."

[19] R. Dennington, T. Keith, J. Millam, Gaussview, Version 5, Semichem Inc., Shawnee Mission, KS, 2009.

[20] A.D. Becke, Density-functional thermochemistry. III. The role of exact exchange, J. Chem. Phys. 98 (1993) 5648-5652.

[21] A.D. Becke, Density-functional thermochemistry. V. Systematic optimization of exchange-correlation functional J. Chem. Phys. 107 (1997) 8554-8560.

[22] REDDY, B. VISHNU THEJA, and CHANDRAMANI CHANDRAKAR. "AN ALTERNATIVE TO ENDOSULFAN: STRUCTURE BASED PHARMACOPHORE MODELING, GLIDE AND MM-GBSA ANALYSIS OF ECDYSONE RECEPTOR AND MOLECULAR DYNAMICS STUDIES." International Journal of Bio-Technology and Research (IJBTR) 5.1, Feb 2015, 1-10

[23] C. Lee, W. Yang, R.G. Parr, Development of the Colle-Salvetti correlation-energy formula into a functional of the electron density Phys. Rev. B 37 (1988) 785-789.

[24] M.H. Jamroz, J.Cz. Dobrowalski, R. Brzozowski, Vibrational Energy Distribution Analysis: VEDA 4 Program, Warasaw, Poland (2004).

[25] G.M. Morris, R. Huey, W. Lindstrom, M.F. Sanner, R.K. Belew, D.S. Goodsell, A.J. Olson, J. Comput. Chem. 30 (16) (2009) 2785-2791.

[26] Discovery Studio 4.5 Guide, Accelrys Inc., San Diego, 2009. http://www.accelrys.com.

[27] Mossaraf Hossain, Renjith Thomas, Y. Sheena Mary, K.S.Resmi, Stevan Armakovic, Sanja J. Armakovic, Ashis Kumar Nanda, G. Vijayakumar, C. Van Alsenoy, Understanding

reactivity of two newly synthetized imidazole derivatives by spectroscopic characterization and computational study, Journal of Molecular Structure 1158 (2018) 176-196.

[28] E.B. Sas, E. Kose, M. Kurt, M. Karabacak, FT-IR, FT-Raman, NMR and UV–Vis spectra and DFT calculations of 5-bromo-2-ethoxyphenylboronic acid (monomer and dimer structures), *Spectrochimica Acta Part A: Molecular and Biomolecular Spectroscopy* (2014), doi: http://dx.doi.org/10.1016/j.saa.2014.08.049

[29] N.B. Colthup, L.H. Daly, S.E. Wiberly, Introduction to IR and Raman Spectroscopy, Academic Press, New York, 1990.

[30] M.Kurt, J Raman Spectrosc. 40(2009) 67-75.

[31] Etem Kose, Ahmet Atac, Fehmi Bardak, The structural and spectroscopic investigation of 2-chloro-3-methylquinoline by DFT method and UV-Vis, NMR and vibrational spectral techniques combined with molecular docking analysis, Journal of Molecular Structure 1163 (2018) 147-160.

[32] Y. S. Mary, C. Y. Panicker, M. Sapnakumari, B. Narayana, B.K. Sarojini, A.A. Al-Saadi, C. V. Alsenoy, J. A. War, H.K. Fun, Infrared spectrum, structural and optical properties and molecular docking study of 3-(4-fluorophenyl)-5-phenyl-4, 5-dihydro-1H-pyrazole-1-carbaldehyde Spectrochim. Acta. 138 (2015) 52**9**–538.

[33] Narayana B, Salian V. V, Sarojini B. K,Jasinski J. P. 1-{3-(4-Chlorophenyl)-5-[4-(propan-2-yl)phenyl]-4,5-dihydro-1H-pyrazol-1-yl}ethanone. Acta Cryst. E70(7) (2014) o781–o781.

[34] S.Gunasekaran & B.Anitha, spectral investigation and normal coordinate analysis of piperazine Indian journal of pure and appl. Phys, 46 (2008) 833-838.

[35] G. Socrates, Infrared Characteristic Group Frequencies, John Wiley and Sons, New York, 1981.

[36] G. Varsanyi , G. Varsanyi , Assignments for Vibrational Spectra of Seven Hundred Benzene Derivatives, Wiley, New York, 1974 .

[37] R.M. Silverstein, G.C. Bassler, T.C. Morril, Spectrometric Identification of Organic Compounds, fifth ed., John Wiley and Sons, Inc., Singapore, 1991.

[38] Abdul-Malek S. Al-Tamimi, Y. Sheena Mary, Pankaj B. Miniyar, Lamya H. Al-Wahaibi, Ali A. El-Emam, Stevan Armakovic, Sanja J. Armakovic, Synthesis, spectroscopic analyses, chemical reactivity and molecular docking study and anti-tubercular activity of pyrazine and condensed oxadiazole derivatives, Journal of Molecular Structure 1164 (2018) 459-469.

[39] D. Lin-Vein, Phys. Rev. 7B (1973) 2600-2626.

[40] B. Smith, Infrared Spectral Interpretation: A Systematic Approach, CRC press, Boca Raton, 1999.

[41] M. Sathish, G. Meenakshi, S. Xavier, S. Sebastian, S. Periandy, NoorAisyah Ahmad, Joazaizulfazli Jamalis, MohdMustaqim Rosli, Hoong-Kun Fun, Synthesis, molecular structure, Hirshfeld surface, spectral investigations and molecular docking study of 3-(5-bromo-2-thienyl)-1-(4-fluorophenyl)-3-acetyl-2-pyrazoline (2) by DFT method, Journal of Molecular Structure 1164 (2018) 420-437.

[42] Y.B. Shankar Rao, M.V.S. Prasad, N. Udaya Sri, V. Veeraiah, Vibrational (FT-IR, FT-Raman) and UV-Visible spectroscopic studies, HOMOeLUMO, NBO, NLO and MEP analysis of Benzyl (imino (1H-pyrazol-1-yl) methyl) carbamate using DFT Calculaions, J. Mol. Struct. 1108 (2016) 567-582.

[43] D.L. Pavia, G.M. Lampman, G.S. Kriz, J.A. Vyvyan, Introduction to Spectroscopy, fifth ed., Cengage Learning India Private Limited, New Delhi, India, 2015.

[44] V.B. Singh, Ab initio and DFT studies of the vibrational spectra of benzofuran and some of its derivatives, Spectrochim. Acta, Part A 65 (2006) 1125-1130.

[45] S. George, Infrared and Raman Characteristic Group Frequencies,Tables and Charts, third ed, Wiley, New York, 2001 .

[46] Y.S. Mary, C.Y. Panicker, P.L. Anto, M. Sapnakumari, B. Narayana, B.K. Sarojini, Spectrochim. Acta 135 (2015) 81-92.

[47] P.K. Murthy, G. Krishnaswamy, S. Armakovic, S.J. Armakovic, P.A. Suchetan, N.R. Desai, V. Suneetha, R. SreenivasaRao, G. Bhargavi, D.B. Arunakumar, Structural and spectroscopic characterization, reactivity study and charge transfer analysis of the newly synthetized 2-(6-hydroxy-1-benzofuran-3-yl) acetic acid, J. Mol. Struct. 1162 (2018) 81-95.

[48] K. Venil, A. Lakshmi, V. Balachandran, B. Narayana, Vinutha V. Salian, FT-IR and FT-Raman investigation, quantum chemical analysis and molecular docking studies of 5-(4-Propan-2-yl)benzylidene)-2-[3-(4-chlorophenyl)-5[4-(propan-2- yl)phenyl-4,5-dihydro-1H-pyrazol-1-yl]-1,3-thiazole-4(5 *H*)-one, Journal of Molecular Structure 1225 (2021) 129070.

[49] S.S. Parveen, M.A. Al-Alshaikh, C.Y. Panicker, A.A. El-Emam, M. Arisoy, O. Temiz-Arpaci, C. Van Alsenoy, J. Mol. Struct. 1115 (2016) 94-104.

[50] M. Tammer, G. Sokrates, Infrared and Raman characteristic group frequencies: tables and charts, Colloid Polym. Sci. 283 (2) (2004) 235.

[51] Shargina Beegum, Sheena Mary Y, C. Yohannan Panicker, Stevan Armakovic, Sanja J. Armakovic, Mustafa Arisoy, Ozlem Temiz-Arpaci, Christian Van Alsenoy, Spectroscopic, antimicrobial and computational study of novel benzoxazole derivative, Journal of Molecular Structure 1176 (2019) 881-894.

[52] M. Karabacak , S. Bilgili , A. Atac , Theoretical study on molecular structure and vibrational analysis included FT-IR, FT-Raman and UV techniques of 2, 4, 5-trimethylbenzoic acid (monomer and dimer structures), Spectrochim. Acta 134 (2015) 598–607.

[53] Abdul-Malek S. Al-Tamimi, Y. Sheena Mary, Hanan M. Hassan, K.S. Resmi, Ali A. El-Emam, B. Narayana, B.K. Sarojini, Study on the structure, vibrational analysis and molecular docking of fluorophenyl derivatives using FT-IR and density functional theory computations, Journal of Molecular Structure 1164 (2018) 172-179.

[54] Harikrishnan, S., and T. J. Bhoopathy. "VIBRATIONAL SPECTROSCOPY INVESTIGATION AND HYBRID COMPUTATIONAL (HF &DFT) ANALYSIS ON THE STRUCTURE OF CHLORZOXAZONE." *Science and Engineering (IJMMSE)* 3.3 (2013): 23-34.

[55] Murtaza Madni, Muhammad Naeem Ahmed, Shahid Hameed, Syed Wadood Ali Shah, Umer Rashid, Khurshid Ayub, M.Nawaz Tahir, Tariq Mahmood, Synthesis, quantum chemical, in vitro acetyl cholinesterase inhibition and molecular docking studies of four new coumarin based pyrazolylthiazolee nuclei, Journal of Molecular Structure 1168 (2018) 175-186.

[56] Kumar, T. Vijaya, and K. V. Ramana. "Investigations and Comparison of Thermogravimetric and Differential Thermal Analysis of Molybdenum Trioxide and its Nanocomposite Powders." *International Journal of Mechanical and Production Engineering Research and Development.* 10 (2020): 6403-6412.

[57] B. Fathima Rizwana, Johanan Christian Prasana, Christina Susan Abraham, S. Muthu, Spectroscopic investigation, hirshfeld surface analysis and molecular docking studies on anti-viral drug entecavir, Journal of Molecular Structure 1164 (2018) 447-458.

[58] P. Rajamani, N. Sundaraganesan, V. Vijayakumar, Maria Susai Boobalan, Mani Jeeva, Synthesis, spectroscopic, computational and molecular docking studies of 1-(pyridin-2-yl amino)methyl napthalene-2-ol, Journal of Molecular Structure 1197 (2019) 417-429.

[59] SRIMURUGAN, R., B. VIJAYA RAMNATH, and C. ELANCHEZHIAN. "AN INVESTIGATION ON MECHANICAL BEHAVIOUR OF NYLON 6-POLYCARBONATE HYBRID COMPOSITE." International Journal of Mechanical and Production Engineering Research and Development (IJMPERD) 8.6, Dec 2018, 525-532

[60] Yusuf Sert, Halil G€okce, Chandra, M. Mahendra, N. Srikantamurthy, Çagrı Çırak, Molecular docking and vibrational spectroscopy studies of (E)-N0-hydroxy-1,3-diphenyl-4,5-dihydro-1H-pyrazole-5- carboximidamide, Journal of Molecular Structure 1184 (2019) 79-91.

[61] Adel S. El-Azab, Y. Sheena Mary, Alaa A.M. Abdel-Aziz, Pankaj B. Miniyar, Stevan Armakovic, Sanja J. Armakovic, Synthesis, spectroscopic analyses (FT-IR and NMR), vibrational study, chemical reactivity and molecular docking study and anti-tubercular activity of condensed oxadiazole and pyrazine derivatives, Journal of Molecular Structure 1156 (2018) 657-674.

[62] F. Weinhold, C. R. Landis, Valency and Bonding: A natural bond orbital Donor – Acceptor perspective, Cambridge University Press, Cambridge, 2005.

[63] R.A. Costa, K.M.T. Oliveira, E.V. Costa, M.L.B. Pinheiro, Vibrational, structural and electronic properties investigation by DFT calculations and molecular docking studies with DNA topoisomerase II of strychnobrasiline type alkaloids: a theoretical approach for potentially bioactive molecules, J. Mol. Struct. 1145 (2017) 254-267.

[64] R.J. Parr, L.V. Szentpaly, S. Liu, "Electrophilicity Index," *Journal of the American chemical society* 121 (1999) 1922-1924.

[65] C. James, A. AmalRaj, R. Reghunathan, I. Hubert Joe, V.S. Jayakumar, J. Raman, Spectrosc. 37 (2006)1381.

[66] Shah, Mehul K., Chetan B. Bhatt, and Jaimin B. Dave. "NIR spectroscopy: Technology ready for food industries applications." *Int. J. Appl. Nat. Sci. IJANS* 5.1 (2016): 129-138.

[67] S. Murugavel, C. Ravikumar, G. Jaabil, Ponnusamy Alagusundaram, Synthesis, crystal structure analysis, spectral investigations (NMR, FTIR, UV), DFT calculations, ADMET studies, molecular docking and anticancer activity of 2-(1-benzyl-5-methyl-1H-1,2,3-triazol-

4-yl)-4- (2-chlorophenyl)-6-methoxypyridine e A novel potent human topoisomerase IIa inhibitor, Journal of Molecular Structure 1176 (2019) 729-742.

[68] Shah, Mehul K., Chetan B. Bhatt, and Jaimin B. Dave. "NIR spectroscopy: Technology ready for food industries applications." *Int. J. Appl. Nat. Sci. IJANS* 5.1 (2016): 129-138.

[69] Maximiliano Martínez-Cifuentes, Boris E. Weiss-L_opez, Leonardo S. Santos, Ramiro Araya-Maturana, Intramolecular hydrogen bond in biologically active o-carbonyl hydroquinones, Molecules 19 (7) (2014) 9354-9368. https://doi.org/10.3390/molecules19079354

[70] www.rcsb.org